Comparison of spatial filters and features for the detection and classification of movement-related cortical potentials in healthy individuals and stroke patients

Jochumsen, Mads; Niazi, Imran Khan; Mrachacz-Kersting, Natalie; Jiang, Ning; Farina, Dario; Dremstrup, Kim

Published in:
Journal of Neural Engineering

DOI (link to publication from Publisher):
10.1088/1741-2560/12/5/056003

Publication date:
2015

Document Version
Accepted author manuscript, peer reviewed version

Comparison of spatial filters and features for the detection and classification of movement-related cortical potentials in healthy individuals and stroke patients

Mads Jochumsen[1], Imran Khan Niazi[1,2,3], Natalie Mrachacz-Kersting[1], Ning Jiang[4], Dario Farina[5] and Kim Dremstrup[1§]

[1]Center for Sensory-Motor Interaction, Department of Health Science and Technology, Aalborg University, Denmark

[2]Center for Chiropractic Research, New Zealand College of Chiropractic, Auckland, New Zealand

[3]Health & Rehabilitation Research Institute, AUT University, New Zealand

[4]Department of Systems Design Engineering, Faculty of Engineering, Centre for Bioengineering & Biotechnology, University of Waterloo, Waterloo, Canada

[5]Department of Neurorehabilitation Engineering, Bernstein Center for Computational Neuroscience, University Medical Center Göttingen, Georg-August University, Göttingen, Germany

[§]Corresponding author

Kim Dremstrup, PhD

Department of Health Science and Technology,

Aalborg University,

Fredrik Bajers vej 7D, D2-212, 9220, Aalborg, Denmark

Tel: + 45 9940 8811

Fax: + 45 9815 4008

Email addresses:

MJ: mj@hst.aau.dk

IKN: imrankn@hst.aau.dk

NMK: nm@hst.aau.dk

NJ: ning.jiang@uwaterloo.ca

Comparison of spatial filters and features for the detection and classification of movement-related cortical potentials in healthy individuals and stroke patients

DF: dario.farina@bccn.uni-goettingen.de

KD: kdn@hst.aau.dk

Abstract

Objective. The possibility of detecting movement-related cortical potentials (MRCPs) at the single trial level has been explored for closing the motor control loop with brain-computer interfaces (BCIs) for neurorehabilitation. A distinct feature of MRCPs is that the movement kinetic information is encoded in the brain potential prior to the onset of the movement which makes it possible to timely drive external devices to provide sensory feedback according to the efferent activity from the brain. The aim of this study was to compare methods for the detection (different spatial filters) and classification (features extracted from various domains) of MRCPs from continuous electroencephalography recordings from executed and imagined movements from healthy subjects (n=24) and attempted movements from stroke patients (n=6) to optimize the performance of MRCP-based BCIs for neurorehabilitation. *Approach.* The MRCPs from four cue-based tasks were detected with a template matching approach and a set of spatial filters, and classified with a linear support vector machine using the combination of temporal, spectral, time-scale, or entropy-based features. *Main results.* The best spatial filter (large Laplacian, LLSF) resulted in a true positive rate of 82±9%, 78±12% and 72±9% (with detections occurring ~200 ms before the onset of the movement) for executed, imagined and attempted movements (stroke patients). The best feature combination (temporal and spectral) led to pairwise classification of 73±9%, 64±10% and 80±12%. When the detection was combined with classification, 60±10%, 49±10% and 58±10% of the movements were both correctly detected and classified for executed, imagined and attempted movements. A similar performance for detection and classification was obtained with optimized spatial filtering. *Significance.* A simple setup with a LLSF is useful

for detecting cued movements while the combination of features from the time and frequency domain can optimize the decoding of kinetic information from MRCPs; this may be used in neuromodulatory BCIs.

Keywords: Movement-related cortical potentials, brain-computer interface, movement kinetics, EEG, signal processing.

1. Introduction

Brain-computer interfaces (BCIs) have been traditionally applied for communication and control purposes (1), but over the past years BCI technology has started to attract attention within the area of neurological rehabilitation after stroke (2,3). Recently, a neuromodulatory protocol was proposed where the cortical activation through cued motor imagination (MI) was paired with timely correlated somatosensory feedback from electrical stimulation of a peripheral nerve (4). The protocol increased the corticospinal excitability of the cortical projections of the target muscle through Hebbian-like plasticity. Induction of plasticity has been correlated with motor learning (5) which is the aim in the rehabilitation process for stroke patients. The protocol proposed by Mrachacz-Kersting et al. was implemented as a self-paced BCI by detecting MI of a specific movement and providing somatosensory feedback from electrical stimulation and passive movement from an ankle-foot orthosis (6,7). The control signal that was used in these studies is known as the movement-related cortical potential (MRCP). It is a slow brain potential that is present in the electroencephalogram (EEG) up to 2 s before the execution and imagination of cued and self-paced voluntary movements (8-11). Besides containing information about when a forthcoming movement is occurring, kinetic information is encoded in the MRCP such as the level of force and speed of the intended movement (11-13). The information about the level of force and speed of a forthcoming movement may be used as input to functional electrical stimulation which then can provide feedback associated to the specific efferent activity from the brain. By decoding kinetic information more

degrees of freedom can be obtained; this opens the possibility of practising different variations (task variability) of a movement type which has been shown to maximize the retention of acquired motor skills and the capability of generalizing relearned movements (14).

The performance of the BCI has been shown to be correlated to the efficacy of the neuromodulatory protocol described above (6). Therefore, the best techniques for detecting MRCPs should be determined as well as the best methods for discriminating variations of specific movements to optimize the performance of BCIs for neurorehabilitation. It has been shown previously that MRCPs can be extracted from the continuous EEG using different methods for pre-processing of the signals and detection algorithms (15-20). These techniques include various types of spatial and temporal filters, data projections, blind source separation, and feature extraction for classification of movements versus an idle state. Moreover, the level of force and speed has been classified from MRCPs associated with executed and imagined movements for different parts of the body and different movement types, such as plantar- and dorsiflexion of the ankle joint (16,21-24), foot and finger tapping (25) and wrist extensions and rotations (26,27). For this classification, various features have been used, such as time-domain features (16,25), band power and power spectral density (25,26,28), time-frequency and time-scale coefficients (21,22,27), and measures of complexity (24). The features from the various domains may contain different discriminative information thus a combination of these may improve the performance of the classifier. The feature extraction techniques are mainly evaluated in a limited number of healthy subjects which makes it difficult to translate the findings to the intended user groups; stroke patients. The inclusion of the intended users may promote the translation of BCI technology from the laboratory to the clinic.

The aim of this study was to investigate the effect of different spatial filters on the detection performance of cue-based MRCPs associated with different kinetic profiles in terms of true positive rate (TPR). The effect of different spatial filters on the TPR has been explored for self-paced MRCPs; however, it has been shown that cue-based and self-paced MRCPs differ in neural generators and signal morphology (29,30). Moreover, the effect of applying different spatial filters was evaluated for classification of movement kinetics of executed and

imagined movements from healthy subjects and attempted movements from stroke patients. Lastly, the optimal types of features to use for classification of movement kinetics were determined.

2. Methods

2.1. Subjects

24 healthy subjects (7 women and 17 men: 27±4 years old) and six stroke patients with lower limb paresis participated in the study (see table 1 for the individual patient information). All procedures were approved by the local ethical committee (N-20100067 and N-20130081), and the participants gave their written informed consent before the experiment.

Table 1: Patient specifications.

Patient	Diagnosis	Affected site	Gender	Age	Days since event
1	Infarction	Left	Female	59	35
2	Infarction	Right	Male	77	46
3	Hemorrhage	Right	Male	54	58
4	Infarction	Right	Male	51	62
5	Infarction	Right	Female	58	46
6	Infarction	Left	Male	38	36

2.2. Experimental protocol

Each subject was seated in a comfortable chair with their right (or affected for the patients) foot fixed to a custom made pedal. Force was recorded from a force transducer mounted to the pedal. At the beginning of the experiment, the maximum voluntary contraction (MVC) was determined followed by 4×50 repetitions of the following tasks of ankle dorsiflexion (see figure 1): i) 0.5 s to reach 20% MVC, ii) 0.5 s to reach 60% MVC, iii) 3 s to reach 20% MVC and iv) 3 s to reach 60% MVC (16).

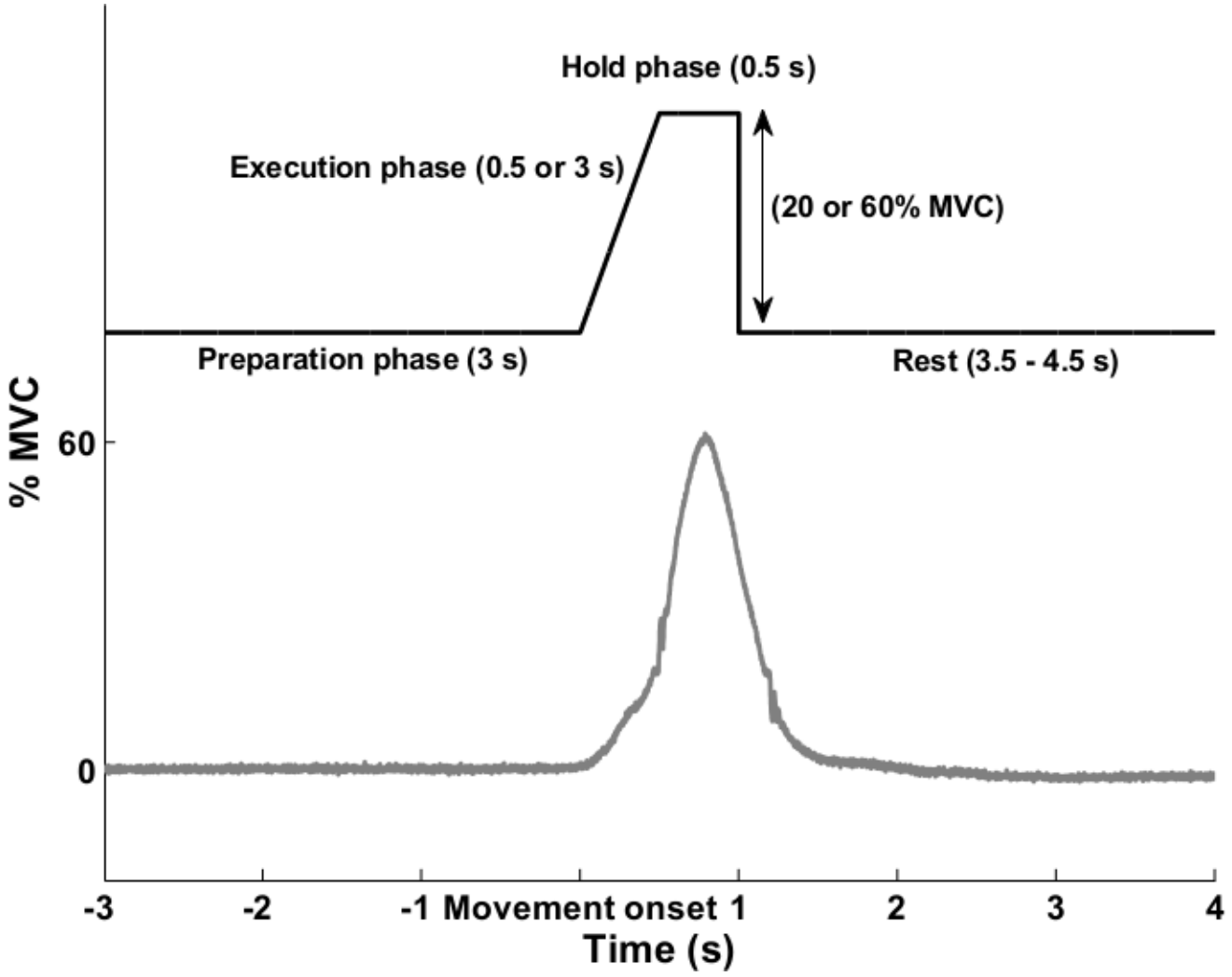

Figure 1: Top: Visual cue that was provided to the subject. A moving cursor (with force as input) indicated when the subjects should initiate the movement and how fast and what level of their MVC to reach. Bottom: Force associated with a movement performed by a representative stroke subject. The same visual cue was presented for subjects performing motor imagination to assist them in timing the onset of the movement; however, no force was produced.

See figure 2 for a grand average of the MRCPs associated with the four tasks. In the following, 0.5 s to reach the desired MVC will be referred to as 'Fast', and 3 s to reach the same will be referred to as 'Slow'. The subjects were constrained to spend the given time to reach the desired level of MVC. To assist them in performing the movements correctly they were visually cued (figure 1) by a custom made program (Knud Larsen, SMI, Aalborg

University). Each movement was separated with 8-10 s and initiated by a digital trigger. The healthy subjects were divided into two sub-groups of 12. One group was asked to perform the tasks while the subjects in the other group imagined the movements. The patients were asked to attempt to perform the tasks. The tasks were randomized in blocks, and ~5 min practice was performed before each task to familiarize the subjects with the tasks. For the subjects performing imagined movements, they practiced motor execution first to recall the kinaesthetic of the movement before practicing the imaginary movements.

Comparison of spatial filters and features for the detection and classification of movement-related cortical potentials in healthy individuals and stroke patients

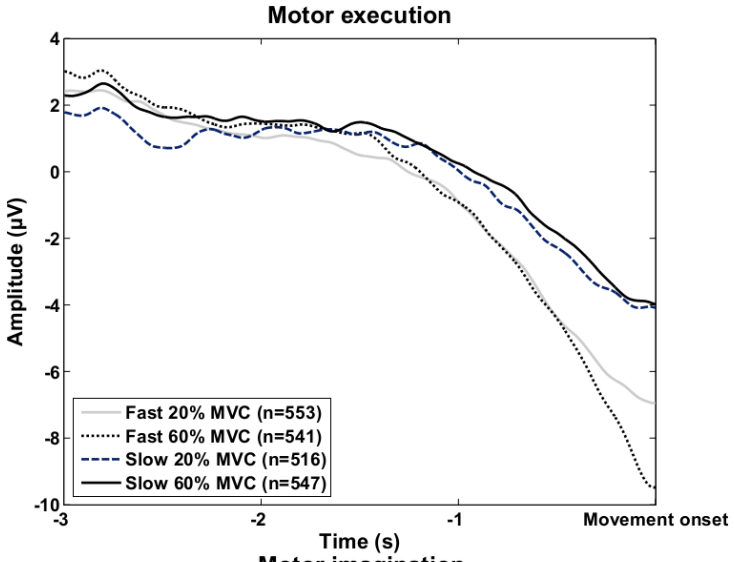

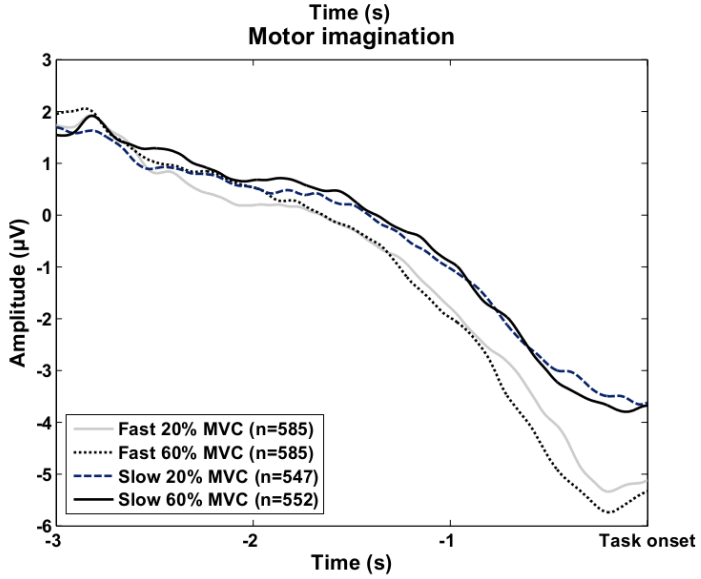

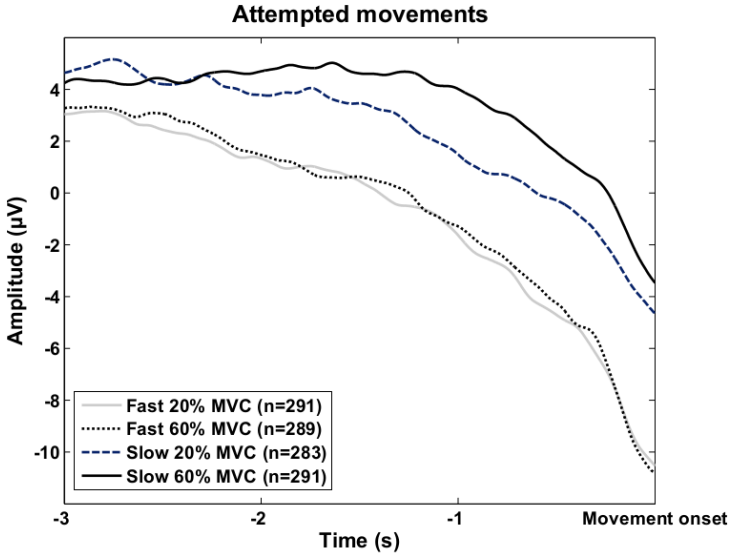

Figure 2: Grand average (across subjects) of the MRCP traces of the four tasks for ME (top), MI (middle) and attempted ME (bottom). The averaged MRCP traces are shown for 3-s epochs prior the onset of the movement or task (for motor imagination). Note the difference in the scaling of the y-axes.

2.3. Signal acquisition

2.3.1.EEG

Continuous EEG was recorded from FP1, F3, Fz, F4, C3, Cz, C4, P3, Pz and P4 according to the International 10-20 system (32 Channel Quick-Cap, Neuroscan and EEG Amplifiers, Numaps Express, Neuroscan). The signals were referenced to the right ear lobe, and ground was placed at nasion. The EEG was sampled with 500 Hz and digitized with 32 bits accuracy. Electrooculography (EOG) was registered from FP1. The impedance of the electrodes was below 5 kΩ during the experiment. The digital trigger from the interface software was sent to the EEG amplifier for epoching the continuous EEG.

2.3.2.Force and MVC

The force was used as input to the program that cued the subjects, so they were provided with visual feedback on their performance (except for the sub-group that imagined the movements). Force was recorded with custom made software (Knud Larsen, SMI, Aalborg University) and sampled with 2000 Hz. The MVC was recorded at the beginning of the experiment. Three MVCs were performed with 60 s break in between each repetition. The highest value was used as the MVC. The onset of each executed movement for the healthy subjects and patients was determined from the force trace. It was identified when all values in a 200 ms window (with a 1-sample shift) exceeded the baseline; then the time point at the beginning of the 200 ms window was used. The baseline was defined as the mean value of the signal 2-4 s before the task onset provided by the visual cue. The movement onset was used to determine the detection latencies and to synchronize all epochs.

2.4. Signal processing

The EEG was band-pass filtered with a 2nd order Butterworth filter from 0.05-10 Hz in the forward and reverse direction for movement detection and for the extraction of temporal features. The remaining features were

extracted from data that were high-pass filtered with a cut-off frequency of 0.05 Hz. To correct for the poor spatial resolution of EEG, the data were spatially filtered. Four spatial filters were compared: Large Laplacian (LLSF), optimized spatial filter (OSF) (15), common average reference (CAR), and common spatial pattern (CSP).

The CAR was calculated for Cz as described in (31). OSF is a data-driven approach that was used to find the filter weights to maximize the signal-to-noise ratio on the training data (15). CSP was used to maximize the distance between signal epochs and noise epochs and was implemented as in (32). Signal epochs were extracted from the movement/task onset and 2 s prior this point; noise epochs were extracted from 5-3 s prior the movement/task onset.

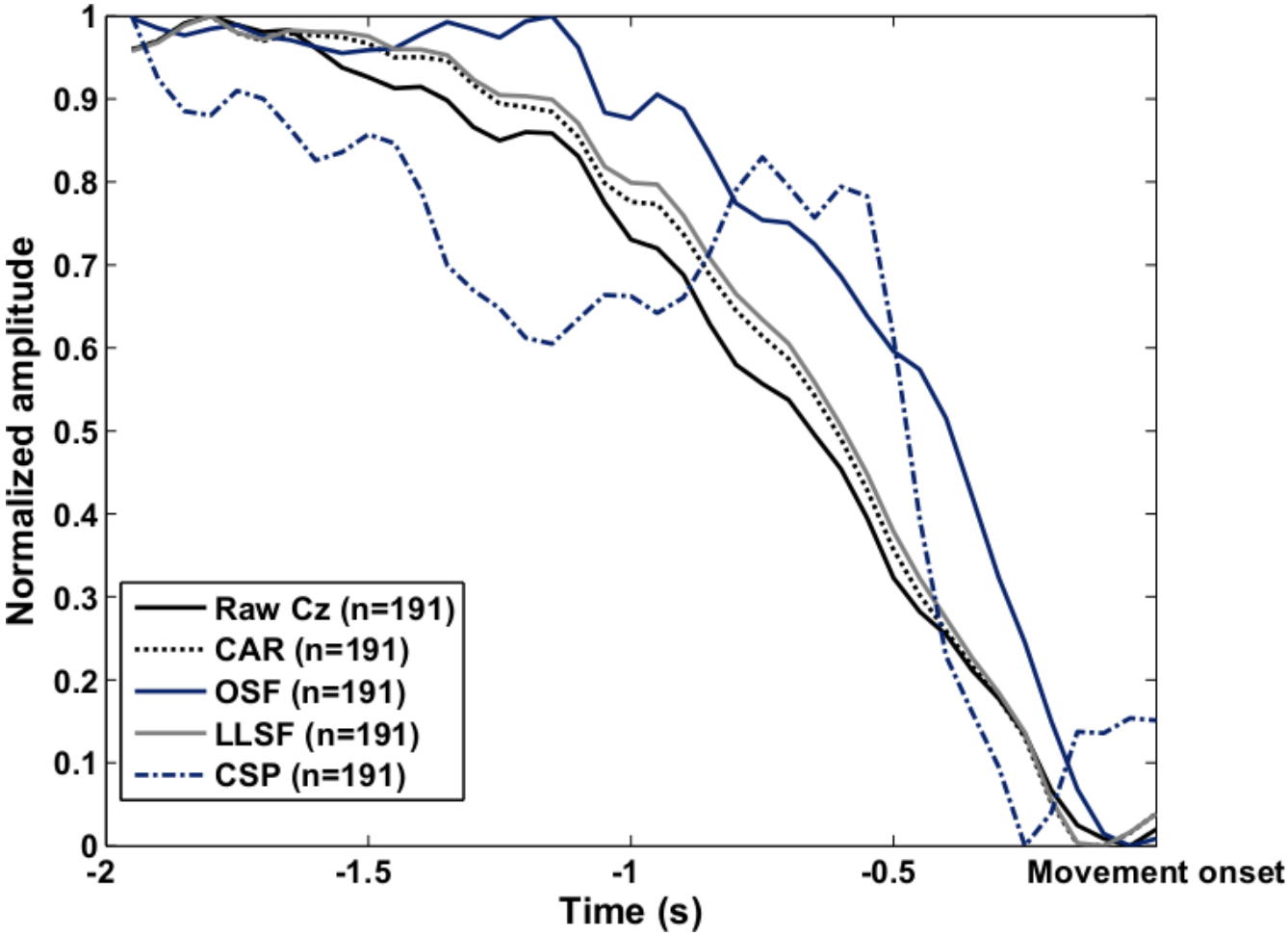

Figure 3: Averaged MRCP across tasks for a representative subject when using the different spatial filters.

2.5. Movement detection

The method for detecting movements was similar to the one proposed by Niazi et al (15) and Jochumsen et al (16). The analysis was performed offline on the continuous EEG recordings. Initially, the data were band-pass filtered and spatially filtered with one of the four filters (LLSF, OSF, CAR or CSP) to obtain a weighted linear combination of the EEG channels. The data set was randomly divided into four parts (four-fold cross-validation); three for training of the detector and one for testing the performance of the constructed detector. For the OSF and CSP, the filter coefficients were calculated on the training set. A template was extracted from the spatially filtered data of the training set by averaging all trials from the peak of maximum negativity and 2 s prior this point (see figure 3). From the training set, a receiver operating characteristics (ROC) curve was obtained to determine the detection threshold. The threshold was selected at the upward convex part of the ROC curve to obtain a trade-off between the number of false positive detections and the TPR. When two out of three consecutive windows exceeded the detection threshold, and EOG activity in FP1 was below the EOG threshold (125 µV), a detection was registered. The detector decision was based on the likelihood ratio (Neyman Pearson lemma) between the template and the weighted linear combination in a 2 s window with a 200 ms shift. The performance of the detector was quantified by the TPR, number of false positive detections per minute (FPs/min), and the detection latency. The detection latency was defined as the time of detection according to the movement onset (for motor execution - ME) or task onset (for MI).

2.6. Feature extraction and selection

All features were extracted from the point of detection to 2 s prior this point.

2.6.1. Temporal features

Six temporal features were extracted for the executed movements, as described previously (16): i) point of maximum negativity, ii) mean amplitude of the 2 s data window, iii+iv) slope and intersection of a linear regression of the data in the 2 s window, v+vi) slope and intersection of a linear regression of the data from the

point of detection and 0.5 s prior this point. For the imaginary movements, the same features were extracted except for the intersections of the two linear regressions. Also, the mean amplitude of the data from the point of detection and 0.5 s prior this point was extracted.

2.6.2.Spectral features

Five spectral features were extracted. Welch's power spectral density estimate was calculated on each epoch using a Hamming window with 50% overlap of the segments. The average power was calculated in the following frequency ranges: i) 0-4 Hz, ii) 4-8 Hz, iii) 8-13 Hz, iv) 13-30 Hz and v) 30-100 Hz. These ranges correspond approximately to the delta, mu, alpha, beta and gamma frequency bands, respectively.

2.6.3.Time-scale features

The marginal distribution of the discrete wavelet transform (DWT) was calculated for 10 different mother wavelets (21). Daubechies 1-10 mother wavelets were used and for each mother wavelet, 10 levels of decomposition were calculated. The marginal distribution was calculated for each level of the decomposition and used as a feature.

2.6.4.Entropy-based features

Four types of entropy were calculated for each epoch and used as features: i) approximate entropy (ApEn) (33), ii) permutation entropy (PeEn) (34,35), iii) sample entropy (SaEn) (36) and iv) constrained sample entropy (CSEn) (37). The false-nearest neighbors' algorithm was used to determine the optimal embedding dimension (m=2) (38). The tolerance for ApEn, PeEn and SaEn was 0.2 x standard deviation of the epoch, and the time lag was 1. For the constrained sample entropy, the tolerance was fixed at 0.2 x standard deviation of all "noise" epochs for the specific task (see section 2.4).

2.6.5.Feature selection

The combination of the features for each of the four feature types (temporal, spectral, time-scale and entropy) was used to classify the task pairs (fast 20% MVC vs fast 60% MVC, etc.). The best combination of features for

each feature type, leading to the highest classification accuracy across the task pairs, was selected. This was followed by an evaluation of classification accuracies for the combination of the optimized feature types. The classification accuracies were obtained using leave-one-out cross-validation and a support vector machine (SVM) with a linear kernel.

2.7. Movement classification

The classification was divided into two main categories: 2-class and 4-class problems. The 2-class classification accuracies were obtained using leave-one-out cross-validation. The classification accuracy for each task pair was calculated (Fast 20% MVC vs. Fast 60% MVC, Fast 20% MVC vs. Slow 20% MVC, etc.). The classification accuracies for the 4-class problem were found by extending the binary SVM to a multi-class SVM using the 'one-vs-one' scheme. A classifier was constructed for each task pair and a test sample was tested by each one. It was labelled according to the class with most votes. The number of correctly classified samples was divided with the number of performed movements in the specific class to obtain the classification accuracy.

2.8. System performance

The system performance was calculated by combining the TPR with the classification accuracy. It is assumed that the two events are independent; therefore, the following formula is used:

$$Performance = \frac{CA(1,2) * [TPR(1) + TPR(2)]}{2}$$

CA(1,2) is the classification accuracy of the task pair, and TPR(1) and TPR(2) are the TPRs for task 1 and 2, respectively. Using the formula, the percentage of correctly detected and classified movements is obtained for the 2-class system. Also, the percentage of correctly detected and misclassified movements is reported; this is calculated by substituting CA(1,2) with its complement. The 4-class performance was calculated by multiplying the classification accuracy (or its complement) with the TPR for the specific task.

2.9. Statistics

Statistical significance was assumed when the p-value < 0.05. For the analysis of variance (ANOVA) tests, significant test statistics were followed up with a post hoc analysis where Bonferroni's correction was applied for multiple pair-wise comparisons.

2.9.1. Detection

A two-way multivariate ANOVA was performed to investigate the effect of the factors; 'spatial filter' and 'movement type', on the dependent variables; averaged TPRs (across tasks), number of FPs/min and detection latency. 'Spatial filter' had four levels: LLSF, OSF, CAR and CSP, and 'movement type' had three levels: ME, MI and attempted ME. A three-way ANOVA was performed with the factors 'spatial filter', 'movement type' and 'task' to investigate the effect on the TPR for each task (Fast 20% MVC, Fast 60% MVC, Slow 20% MVC and Slow 60% MVC).

2.9.2. Classification and system performance

A three-way ANOVA was performed to investigate if the averaged classification accuracies (across task pairs) differed when using the different spatial filters and feature extraction techniques for the movement types. The factors were 'movement type', 'spatial filter' and 'feature type' with four levels: temporal, spectral, entropy and time-scale. Also, a two-way multivariate ANOVA was performed to test if the classification accuracies and system performance differed for the three movement types when the signals were processed with the different spatial filters. The factors were 'movement type' and 'spatial filter'.

3. Results

The results are summarized in table 2, 3 and 4.

3.1. Detection

On average (across different tasks), the highest TPRs were obtained for LLSF (table 2), although for ME, OSF resulted in the greatest TPR. On average (across tasks) with the LLSF, 82±9%, 78±12% and 72±9% of the movements were correctly detected for ME, MI and attempted ME, respectively. When investigating the

averaged TPRs, no significant interaction was observed between spatial filters and movement types ($F_{(6,119)}$=0.71;P=0.65). However, a significant effect of spatial filter ($F_{(3,119)}$=5.03;P=0.003) was found where the LLSF outperformed CSP. For the movement types ($F_{(2,119)}$=15.29;P=0.000001), all three types were different.

For the number of FPs/min there was an interaction between the type of spatial filter and movement type ($F_{(6,119)}$=3.78;P=0.002). The main effects of spatial filter ($F_{(3,119)}$=4.95;P=0.003) and movement type ($F_{(2,119)}$=10.87;P=0.00005) were significant where LLSF and OSF led to less FPs/min compared to CSP, and ME and MI were lower than attempted ME (see table 2). For the detection latencies, no significant interaction was observed between spatial filter and movement type ($F_{(6,119)}$=1.52;P=0.18), but the main effects of spatial filter ($F_{(2,119)}$= 5.06;P=0.003) and movement type ($F_{(2,119)}$=19.11;P=0.007*10^{-8}) were significant. The detection of movements occurred earlier with LLSF, OSF and CAR compared to CSP, and when ME or MI was performed compared to attempted movements.

To investigate if the TPRs were different for the four tasks a three-way ANOVA was performed. No differences were found; the interaction of movement types, spatial filter and tasks was not significant ($F_{(18,479)}$=0.45;P=0.98). In summary, the best detection performance was obtained with the LLSF, but it was not significantly different from OSF and CAR.

Table 2: The TPR for movement detection of ME, MI and attempted ME is presented. The results are presented (mean ± standard deviation across subjects) for different spatial filters.

Motor execution **Healthy subjects**	**LLSF [%]**	**OSF [%]**	**CAR [%]**	**CSP [%]**
Task				
Fast 20% MVC	83±6	84±8	72±7	77±15
Fast 60% MVC	87±10	86±11	76±9	80±14
Slow 20% MVC	76±9	79±10	69±8	72±11
Slow 60% MVC	81±8	82±9	74±14	81±14
Mean across tasks	82±9	83±9	78±14	73±10
FPs/min	1.1±0.7	1.1±0.7	1.5±0.9	2.6±0.8
Detection latency [ms]	-297±108	-244±125	-297±108	-269±139
Motor imagery **Healthy subjects**				

Task				
Fast 20% MVC	76±13	73±13	71±13	68±14
Fast 60% MVC	78±9	72±13	71±12	68±16
Slow 20% MVC	78±11	69±9	71±16	73±10
Slow 60% MVC	79±13	69±11	74±17	75±13
Mean across tasks	78±12	71±12	72±15	71±13
FPs/min	1.1±0.4	1.3±0.7	1.3±0.5	1.5±0.7
Detection latency [ms]	-209±84	-232±133	-236±99	-169±115
Attempted movements Stroke patients				
Task				
Fast 20% MVC	70±8	65±15	61±9	60±20
Fast 60% MVC	73±8	73±10	65±5	62±15
Slow 20% MVC	73±9	60±16	67±9	63±17
Slow 60% MVC	74±11	72±10	72±11	56±18
Mean across tasks	72±9	67±13	66±8	60±17
FPs/min	1.7±0.1	2±0.3	1.8±0.3	2.3±0.3
Detection latency [ms]	-96±44	-59±113	-64±76	-28±120
	Mean±SD	**Mean±SD**	**Mean±SD**	**Mean±SD**

3.2. Classification and system performance

The classification accuracies for the optimal features for each feature type and the combination of features are presented in table 3. The difference in classification accuracies was tested for the different spatial filters, feature types and movement types. The interaction of the three factors was not significant ($F_{(6,479)}$=1.41;P=0.12), but the effect of feature type ($F_{(3,479)}$=107.24;P=0.07*10^{-50}) and movement type ($F_{(2,479)}$=28.85;P=0.02*10^{-10}) was significant. The classification accuracies associated with the time-scale features were lower than the other three feature types, and those obtained for MI were lower than ME and attempted ME. No difference was found in the classification accuracies when using the different spatial filters.

Table 3: The classification accuracies (CA) associated with the selected features are presented for ME, MI and attempted ME from stroke patients. The order of the features is the same as presented in the Methods section. Also, the classification accuracies are presented for the optimized feature combination. The results are presented for each of the spatial filtering techniques. ‘Temp’: Temporal, ‘Spec’: Spectral, ‘Ent’: Entropy and ‘Ti-Sc’: Time-Scale.

Comparison of spatial filters and features for the detection and classification of movement-related cortical potentials in healthy individuals and stroke patients

Large Laplacian spatial filter				
Feature Type	Selected features	CA across tasks [%] Mean±SD	Optimal feature type combination	CA across tasks [%] Mean±SD
Temp	[1-4,6] / [1-3,5] / [1-4,6]	73±5 / 62±3 / 80±6	ME: [Temp+Spec]	73±9 / 52±14
Spec	[1-3,5] / [1-4] / [2,3,5]	66±3 / 60±1 / 58±3	MI: [Temp+Spec]	64±10 / 37±13
Ent	[1,3,4] / [1,4] / [1,4]	61±4 / 58±3 / 58±4	Stroke: [Temp+Spec]	80±12 / 61±19
Ti-Sc	[db1]/ [db4]/ [db4]	52±3 / 52±2 / 51±1		
	ME/MI/Stroke	**ME/MI/Stroke**		**2-class / 4-class**

Optimized spatial filter				
Feature Type	Selected features	CA across tasks [%] Mean±SD	Optimal feature type combination	CA across tasks [%] Mean±SD
Temp	[1,3,4] / [1,3-5] / [1,3,5,6]	65±5 / 61±5 / 69±5	ME: [Temp+Spec+Ent]	75±14 / 51±19
Spec	[1,3-5] / [1,4,5] / [1,4,5]	71±4 / 71±6 / 71±6	MI: [Temp+Spec]	66±11 / 40±15
Ent	[3,4] / [1,2,4] / [1,4]	68±4 / 60±3 / 67±7	Stroke: [Temp+Spec+Ent]	77±14 / 57±20
Ti-Sc	[db6]/ [db7]/ [db6]	52±3 / 51±2 / 52±1		
	ME/MI/Stroke	**ME/MI/Stroke**		**2-class / 4-class**

Common average reference filter				
Feature Type	Selected features	CA across tasks [%] Mean±SD	Optimal feature type combination	CA across tasks [%] Mean±SD
Temp	[1,3,4,6] / [1-4] / [1-4]	65±4 / 61±4 / 72±6	ME: [Temp+Spec+Ent]	72±11 / 48±16
Spec	[1,2,4,5] / [1,2,4,5] / [1,2,4,5]	66±3 / 58±2 / 67±5	MI: [Temp+Spec+Ent]	64±9 / 39±14
Ent	[3,4] / [1,2,4] / [1,3,4]	63±5 / 60±2 / 66±5	Stroke: [Temp+Spec+Ent]	77±13 / 55±18
Ti-Sc	[db1]/ [db1]/ [db1]	52±2 / 51±3 / 53±1		
	ME/MI/Stroke	**ME/MI/Stroke**		**2-class / 4-class**

Common spatial pattern filter				
Feature Type	Selected features	CA across tasks [%] Mean±SD	Optimal feature type combination	CA across tasks [%] Mean±SD
Temp	[1,3,5,6] / [1,2] / [1-3,5,6]	57±2 / 58±2 / 62±3	ME: [Spec+Ent]	73±14 / 50±20
Spec	[1-5] / [1,3-5] / [1,3-5]	72±3 / 74±5 / 74±5	MI: [Temp+Spec]	67±10 / 42±15
Ent	[1,2,4] / [1,2,4] / [2-4]	68±2 / 63±1 / 71±5	Stroke: [Temp+Spec+Ent]	77±10 / 56±15
Ti-Sc	[db1]/ [db8]/ [db6]	52±3 / 51±2 / 52±1		
	ME/MI/Stroke	**ME/MI/Stroke**		**2-class / 4-class**

Next, it was tested with a multivariate ANOVA if the optimized classification accuracies differed when pre-processing was performed with the different spatial filters for the three movement types. No significant

interaction was observed ($F_{(6,239)}$=0.34;P=0.91). The effect of movement type was significant ($F_{(2,239)}$=19.46;P=0.02*10^{-6}), and it was found that different classification accuracies were obtained for each movement type with attempted ME being higher than ME and MI. For the system performance, when the TPR was combined with the classification accuracies, there was no significant interaction between the factors in the multivariate ANOVA ($F_{(6,239)}$=0.89;P=0.50). The effect of movement types was significant ($F_{(2,239)}$=18.33;P=0.04*10^{-6}) where better performance was obtained for ME and attempted ME compared to MI.

Table 4: Averaged system performance (across subjects and task pairs/tasks) for each spatial filter and movement type; this is reported for a 2-class and 4-class system. The percentage of correctly detected and classified movements is reported as well as the percentage of correctly detected and incorrectly classified movements.

	System performance		
Spatial filter: # of classes	**TPR*CA / TPR*(1-CA)** ***ME – Healthy subjects***	**TPR*CA / TPR*(1-CA)** ***MI – Healthy subjects***	**TPR*CA / TPR*(1-CA)** ***ME – Stroke patients***
LLSF: 2-class	60±10 / 22±8	49±10 / 29±8	58±10 / 14±9
OSF: 2-class	61±12 / 21±12	47±11 / 24±8	52±11 / 15±10
CAR: 2-class	56±11 / 25±9	46±10 / 26±7	51±9 / 16±9
CSP: 2-class	53±12 / 20±10	47±10 / 24±8	46±13 / 14±7
LLSF: 4-class	42±13 / 39±12	28±11 / 49±13	44±15 / 28±14
OSF: 4-class	42±15 / 40±16	29±12 / 42±12	38±15 / 29±15
CAR: 4-class	37±14 / 41±14	28±11 / 44±13	36±12 / 30±12
CSP: 4-class	36±15 / 36±15	30±13 / 41±13	34±12 / 27±11
	Mean±SD	**Mean±SD**	**Mean±SD**

4. Discussion

In general, the highest TPRs and lowest number of FPs/min were obtained using a LLSF and OSF. The optimal features to use for classifying the movement kinetics were the combination of temporal and spectral features. The system performance for healthy subjects was not significantly different from the stroke patients.

4.1. Detection

The highest TPRs were obtained for the fast movements when the healthy subjects performed the movements; this is in agreement with previous findings (16). On the contrary, the TPRs for slow movements when

performing MI and attempted movements were similar or slightly larger than the TPRs for fast movements. This is a bit surprising since the fast movements have larger signal-to-noise ratios compared to the slow movements (see figure 2) (11). Also, it is surprising that the TPRs for the stroke patients were lower than MI for healthy subjects when comparing the grand averages of the two movement types in figure 2; the amplitudes of the MRCPs were larger for the attempted movements compared to MI. Some of the patients had difficulties in relaxing between the movements leading to more FPs/min; therefore the detection threshold was increased to avoid too many FPs/min. The TPR (~80%), number of FPs/min (~1-3) and detection latencies of the detector are in the range of what has been reported previously for ME (15-17,19,20). The slight difference in detection latencies between cued and self-paced movements can be explained by the morphological difference between the signals (30). For MI, a higher TPR (~78%) was obtained compared to previous studies where 65-75% was obtained (6,7,15). Also, the performance of the stroke patients was better than previously reported (~60%) (15). The improved performance may be due to the fact that the healthy subjects and patients were visually cued (39).

The TPRs when using LLSF and OSF were higher compared to CSP processed data. This is consistent with another study where the effect of spatial filtering with OSF, LLSF and CSP was compared for self-paced executed movements (15). The reason for the lower performance of CSP may be due to too little training data to calculate optimal filter coefficients; also, the performance of OSF may be optimized with more training data since these techniques are data-driven approaches. In the current study, the performance of using OSF and LLSF was not different, on the contrary to the findings in Niazi et al. (2011) where OSF was associated with greater TPRs. This can possibly be due to the differences in signal morphology for cue-based and self-paced movements as well as the fact that the movements were performed with different kinetic profiles, which also affect signal morphology (see figure 2) (11,30).

4.2. Feature extraction and classification

It was found that the temporal features were the most discriminative, but the performance was slightly improved when information from the spectral domain and entropy-based features were incorporated. The combination of features from the time and frequency domain has previously been reported for discrimination of different levels of speed for imagined hand movements (26). The performance of the classifiers for ME and MI was comparable to previous studies using temporal (~75%, ME), spectral (~65-70% for fast vs. slow MI) and entropy-based features (~60%, ME) (16,24,40). However, the performance obtained with the time-scale based features using various Daubechies mother wavelets was lower compared to the findings when using parameterized and optimized mother wavelets with more data available for feature extraction (~70-80%) (21-23,27). The classification accuracies obtained from the stroke patients were surprisingly higher than those obtained from the healthy subjects. It is indicated in figure 2 that the attempted movements may be more separable than at least MI. The difference between the classification accuracies of attempted movements and ME may be explained by the amount of information that was available for feature extraction (16). For attempted movements, data until 96±44 ms before the movement onset were used for feature extraction compared to 297±108 ms for ME (see the separation between the average MRCPs around the movement onset in figure 2). The classification accuracies for the 2-class and 4-class problems were above the chance level reported with a confidence interval corresponding to a significance level of α=5% (41).

In this study, subject independent features (and the combination of these) were used, but to optimize the performance subject-dependent features could be extracted. To avoid large dimensionalities of the feature vectors, different feature selection techniques could be used to select the optimal feature set for the specific subject. This approach requires more training of the system.

4.3. Implications

The findings indicate that a simple LLSF can be used for pre-processing the data to obtain a relatively high detection performance and that the classification of movement kinetics can be performed with subject

independent temporal and spectral features. The limited number of channels, simple pre-processing and subject independent features indicate that the system can be implemented online and potentially moved out of the laboratory. The performance of the detector is in the range of what has previously been reported for inducing plasticity (6). When detection is combined with classification, however, the performance needed to induce plastic changes is not known as well as the effect of providing incorrect feedback as a result of incorrect classification. With the current performance of the detector, stroke patients may use such a BCI system for rehabilitation, and it may be possible to extend the detector with classification of movement kinetic information, so more degrees of freedom are obtained. This can potentially be used to introduce task variability in the training and provide sensory feedback according to the efferent activity of the brain; however, the effect of this needs to be addressed.

4.4. Limitations

The analysis was performed offline; however, due the simplicity of the detector and classifier it is feasible to implement them in an online system. The classification accuracies may be more variable using an online system due to the variation in the detection latencies of the movements. This may reduce or increase the amount of discriminative information that can be used for classification. The detection threshold may be modified to tune the detection latency, so it will be reduced (~50-100 ms before the movement onset) which is needed to induce plasticity (4). Modifying the threshold in this way will reduce the number of FPs/min, but also the TPR will be reduced. The system performance of the 2-class systems is in the range to be used for asynchronous control purposes; however, the performance of the 4-class system is not in that range. To reach that level in performance, the number of classes may be reduced from four to three.

5. Conclusion

This study demonstrates that the best detection performance was obtained with LLSF and OSF across tasks and movement types. Also, it was found that the discrimination between movement kinetics can be optimized by combining features extracted from the time and frequency domain. Based on the performance of the stroke

patients, it is feasible to implement a multiclass MRCP-based BCI for stroke rehabilitation where movements can be detected and kinetic information decoded.

Acknowledgments

The authors would like to thank Helle Rovsing Møller Jørgensen from Brønderslev Neurological Rehabilitation Center for recruiting the stroke patients and Rasmus Wiberg Nedergaard and Muhammad Samran Navid for assistance in the data collection. This work was supported by the Danish Technical Research Council.

The authors declare no competing financial interests.

References

(1) Wolpaw JR, Birbaumer N, McFarland DJ, Pfurtscheller G, Vaughan TM. Brain-computer interfaces for communication and control. Clinical neurophysiology 2002;113(6):767-791.

(2) Daly JJ, Wolpaw JR. Brain-computer interfaces in neurological rehabilitation. The Lancet Neurology 2008;7(11):1032-1043.

(3) Grosse-Wentrup M, Mattia D, Oweiss K. Using brain-computer interfaces to induce neural plasticity and restore function. Journal of Neural Engineering 2011;8(2):025004.

(4) Mrachacz-Kersting N, Kristensen SR, Niazi IK, Farina D. Precise temporal association between cortical potentials evoked by motor imagination and afference induces cortical plasticity. J Physiol (Lond) 2012;590(7):1669-1682.

(5) Pascual-Leone A, Dang N, Cohen LG, Brasil-Neto JP, Cammarota A, Hallett M. Modulation of muscle responses evoked by transcranial magnetic stimulation during the acquisition of new fine motor skills. J Neurophysiol 1995;74:1037-1037.

(6) Niazi IK, Kersting NM, Jiang N, Dremstrup K, Farina D. Peripheral Electrical Stimulation Triggered by Self-Paced Detection of Motor Intention Enhances Motor Evoked Potentials. IEEE transaction on neural systems and rehabilitation engineering 2012;20(4):595-604.

(7) Xu R, Jiang N, Mrachacz-Kersting N, Lin C, Asin G, Moreno J, et al. A Closed-Loop Brain-Computer Interface Triggering an Active Ankle-Foot Orthosis for Inducing Cortical Neural Plasticity. Biomedical Engineering, IEEE Transactions on 2014;20(4):2092-2101.

(8) Walter WG, Cooper R, Aldridge VJ, McCallum WC, Winter AL. Contingent negative variation: An electric sign of sensorimotor association and expectancy in the human brain. Nature (Lond.) 1964;203:380-384.

(9) Kornhuber HH, Deecke L. Hirnpotentialänderrungen beim Menschen vor und nach Willkürbewegungen, dargestellt mit Magnetbandspeicherung und Rüchwärtsanalyse. Pflügers Arch. ges. Physiol. 1964;281(52).

(10) Shibasaki H, Hallett M. What is the Bereitschaftspotential? Clinical Neurophysiology 2006;117(11):2341-2356.

(11) Nascimento OF, Dremstrup Nielsen K, Voigt M. Movement-related parameters modulate cortical activity during imaginary isometric plantar-flexions. Experimental brain research 2006;171(1):78-90.

(12) Nascimento OF, Dremstrup Nielsen K, Voigt M. Relationship between plantar-flexor torque generation and the magnitude of the movement-related potentials. Experimental Brain Research 2005;160(2):154-165.

(13) Siemionow V, Yue GH, Ranganathan VK, Liu JZ, Sahgal V. Relationship between motor activity-related cortical potential and voluntary muscle activation. Experimental Brain Research 2000;133(3):303-311.

(14) Krakauer JW. Motor learning: its relevance to stroke recovery and neurorehabilitation. Curr Opin Neurol 2006;19(1):84-90.

(15) Niazi IK, Jiang N, Tiberghien O, Nielsen JF, Dremstrup K, Farina D. Detection of movement intention from single-trial movement-related cortical potentials. Journal of Neural Engineering 2011;8(6):066009.

(16) Jochumsen M, Niazi IK, Mrachacz-Kersting N, Farina D, Dremstrup K. Detection and classification of movement-related cortical potentials associated with task force and speed. Journal of neural engineering 2013;10(5):056015.

(17) Xu R, Jiang N, Lin C, Mrachacz-Kersting N, Dremstrup K, Farina D. Enhanced Low-latency Detection of Motor Intention from EEG for Closed-loop Brain-Computer Interface Applications. Biomedical Engineering, IEEE Transactions on 2013;61(2):288-296.

(18) Bai O, Rathi V, Lin P, Huang D, Battapady H, Fei D, et al. Prediction of human voluntary movement before it occurs. Clinical Neurophysiology 2011;122(2):364-372.

(19) Lew E, Chavarriaga R, Silvoni S, Millán JR. Detection of self-paced reaching movement intention from EEG signals. Frontiers in neuroengineering 2012;5:13.

(20) Niazi IK, Jiang N, Jochumsen M, Nielsen JF, Dremstrup K, Farina D. Detection of movement-related cortical potentials based on subject-independent training. Med Biol Eng Comput 2013;51(5):507-512.

(21) Farina D, Nascimento OFd, Lucas M, Doncarli C. Optimization of wavelets for classification of movement-related cortical potentials generated by variation of force-related parameters. J Neurosci Methods 2007;162(1–2):357-363.

(22) Gu Y, Nascimento OF, Lucas MF, Farina D. Identification of task parameters from movement-related cortical potentials. Medical biological engineering computing 2009;47(12):1257-1264.

(23) Omar Feix do Nascimento, Farina D. Movement-Related Cortical Potentials Allow Discrimination of Rate of Torque Development in Imaginary Isometric Plantar Flexion. Biomedical Engineering, IEEE Transactions on 2008;55(11):2675-2678.

(24) Jochumsen M, Niazi IK, Farina D, Dremstrup K. Classifying Speed and Force From Movement Intentions Using Entropy and a Support Vector Machine. Proceedings of the Fifth International Brain-Computer Interface Meeting 2013 2013.

(25) Fu Y, Xu B, Pei L, Li H. Time Domain Features for Relationship between Speed and Slow Potentials Activity during Periodic Movement and Motor Imagery at Fast and Slow for BCRI. Procedia Environmental Sciences 2011;8(0):498-505.

(26) Gu Y, Dremstrup K, Farina D. Single-trial discrimination of type and speed of wrist movements from EEG recordings. Clinical Neurophysiology 2009 8;120(8):1596-1600.

(27) Gu Y, Farina D, Murguialday AR, Dremstrup K, Montoya P, Birbaumer N. Offline identification of imagined speed of wrist movements in paralyzed ALS patients from single-trial EEG. Frontiers in Neuroscience 2009;3(0).

(28) Fu Y, Xu B, Pei L, Li H. Event-related perturbation in spectral power and in potentials during periodic fast and slow motor imagination for brain-controlled robots interface. Robotics and Biomimetics (ROBIO), 2010 IEEE International Conference on 2010:1299-1304.

(29) Lu M, Arai N, Tsai C, Ziemann U. Movement related cortical potentials of cued versus self-initiated movements: Double dissociated modulation by dorsal premotor cortex versus supplementary motor area rTMS. Hum Brain Mapp 2011;33(4):824-839.

(30) Jankelowitz S, Colebatch J. Movement-related potentials associated with self-paced, cued and imagined arm movements. Experimental brain research 2002;147(1):98-107.

(31) McFarland DJ, McCane LM, David SV, Wolpaw JR. Spatial filter selection for EEG-based communication. Electroencephalogr Clin Neurophysiol 1997;103(3):386-394.

(32) Kawanabe M, Vidaurre C, Blankertz B, Müller K-. A maxmin approach to optimize spatial filters for eeg single-trial classification. Lecture Notes in Computer Science (including subseries Lecture Notes in Artificial Intelligence and Lecture Notes in Bioinformatics) 2009;5517 LNCS(PART 1):674-682.

(33) Pincus SM. Approximate entropy as a measure of system complexity. Proceedings of the National Academy of Sciences 1991 March 15;88(6):2297-2301.

(34) Bandt C, Pompe B. Permutation entropy: A natural complexity measure for time series. Phys Rev Lett 2002;88(17):174102.

(35) Li X, Ouyang G, Richards DA. Predictability analysis of absence seizures with permutation entropy. Epilepsy Res 2007;77(1):70-74.

(36) Richman JS, Moorman JR. Physiological time-series analysis using approximate entropy and sample entropy. American Journal of Physiology - Heart and Circulatory Physiology 2000 June 01;278(6):H2039-H2049.

(37) Kamavuako EN, Farina D, Yoshida K, Jensen W. Estimation of grasping force from features of intramuscular EMG signals with mirrored bilateral training. Ann Biomed Eng 2012;40(3):648-656.

(38) Sprott JC, Sprott JC. Chaos and time-series analysis. : Oxford University Press Oxford; 2003.

(39) Heremans E, Helsen WF, De Poel HJ, Alaerts K, Meyns P, Feys P. Facilitation of motor imagery through movement-related cueing. Brain Res 2009;1278:50-58.

(40) Yunfa Fu, Baolei Xu, Lili Pei, Hongyi Li. Reactive Rhythm Activities and Offline Classification of Imagined Speeds of Finger Movements. Bioinformatics and Biomedical Engineering, (iCBBE) 2011 5th International Conference on 2011:1-5.

(41) Müller-Putz GR, Scherer R, Brunner C, Leeb R, Pfurtscheller G. Better than random? A closer look on BCI results. International Journal of Bioelectromagnetism 2008;10(1):52-55.